The chromosome 3p21.3-encoded gene, *LIMD1*, is a critical tumor suppressor involved in human lung cancer development

Tyson V. Sharp[a], Ahmad Al-Attar[b,1], Daniel E. Foxler[a,1], Li Ding[c], Thomas Q. de A. Vallim[a], Yining Zhang[a], Hala S. Nijmeh[a], Thomas M. Webb[a], Andrew G. Nicholson[d], Qunyuan Zhang[e], Aldi Kraja[e], Ian Spendlove[b], John Osborne[c], Elaine Mardis[c,e], and Gregory D. Longmore[f,2]

[a]School of Biomedical Sciences, Queen's Medical Centre, University of Nottingham Medical School, Nottingham NG7 2UH, United Kingdom; [b]Academic and Clinical Departments of Oncology, University of Nottingham, Nottingham NG5 1PB, United Kingdom; [d]Department of Histopathology, Royal Brompton Hospital, London SW3 6NP, United Kingdom; [c]Department of Genetics, Genome Sequencing Center, and [e]Division of Statistical Genomics, Washington University School of Medicine, St. Louis, MO 63108; and [f]Departments of Medicine and Cell Biology, Washington University, St Louis, MO 63110

Edited by George Klein, Karolinska Institutet, Stockholm, Sweden, and approved October 7, 2008 (received for review May 23, 2008)

Loss of heterozygosity (LOH) and homozygous deletions at chromosome 3p21.3 are common in both small and nonsmall cell lung cancers, indicating the likely presence of tumor suppressor genes (TSGs). Although genetic and epigenetic changes within this region have been identified, the functional significance of these changes has not been explored. Concurrent protein expression and genetic analyses of human lung tumors coupled with functional studies have not been done. Here, we show that expression of the 3p21.3 gene, *LIMD1*, is frequently down-regulated in human lung tumors. Loss of LIMD1 expression occurs through a combination of gene deletion, LOH, and epigenetic silencing of transcription without evidence for coding region mutations. Experimentally, *LIMD1* is a bona fide TSG. *Limd1*$^{-/-}$ mice are predisposed to chemical-induced lung adenocarcinoma and genetic inactivation of *Limd1* in mice heterozygous for oncogenic K-Ras^{G12D} markedly increased tumor initiation, promotion, and mortality. Thus, we conclude that *LIMD1* is a validated chromosome 3p21.3 tumor-suppressor gene involved in human lung cancer development. LIMD1 is a LIM domain containing adapter protein that localizes to E-cadherin cell–cell adhesive junctions, yet also translocates to the nucleus where it has been shown to function as an RB corepressor. As such, LIMD1 has the potential to communicate cell extrinsic or environmental cues with nuclear responses.

LIM proteins | retinoblastoma | K-Ras G12D | epigenetic silencing | tumor suppressor genes

Within chromosome 3p are several TSG regions (1–3). Nine homozygous deletion regions have been described, four of which were found in lung tumors. The chromosome 3 common eliminated region 1 (C3CER1; also called CER1) on chromosome 3p21.3 (4, 5) is one of the putative tumor-suppressor regions identified by the "elimination test," a functional test system that identifies regularly lost (eliminated) chromosome segments in microcell hybrid-derived SCID tumors (6). C3CER1 (megabases 43.32–45.74) is located between 2 such regions, AP20 and LUCA (7, 8). Deletions in this chromosome 3p region are a common event in solid malignancies including breast, gastric, colorectal, ovarian, and renal (5). Furthermore, C3CER1 loss of heterozygosity (LOH) exceeds 90% in lung tumors compared with the putative TSG *FHIT* (65%) and the TSG *VHL* (72%) (5), which map at 3p14.2 and 3p25.3, respectively. In addition, deletions in 3p have been identified in lung adenocarcinomas (ADC) via the tumor sequencing project initiative (3). Therefore, because deletion in this region is a common event in lung tumors, chromosome 3p is under intense study for the identification of putative TSGs

The ≈2.4-Mb C3CER1 region contains ≈32 genes (2). The gene for the LIM domains containing 1 *LIMD1* is a putative TSG encoded within C3CER1. LIMD1 interacts with the retinoblastoma protein (pRB), inhibits E2F-mediated transcription, and suppresses expression of the majority of genes with E2F1-responsive elements (9). Moreover, forced expression of LIMD1 in A549 lung tumor cell line blocks tumor growth in vitro and in vivo (9). Here, we show that expression of the 3p21.3 gene, *LIMD1*, is frequently down-regulated in human lung tumors. Genetic analysis indicates that this occurs through a combination of somatic gene deletion, LOH, and epigenetic silencing of transcription, without evidence for coding region mutations. Finally we also demonstrate that *LIMD1* is a bona fide TSG. *Limd1*$^{-/-}$ mice are predisposed to chemical-induced lung adenocarcinoma, and genetic inactivation of *Limd1* in mice heterozygous for oncogenic K-Ras (G12D) markedly increased lung tumor initiation, promotion, and mortality rate.

Results and Discussion

LIMD1 Protein Is Expressed in Human Bronchial and Alveolar Epithelial Cells. Using a highly specific anti-LIMD1 monoclonal antibody (9), we asked whether and where LIMD1 was expressed in normal lung. Immunohistochemical (IHC) staining showed high-level expression in ciliated pseudostriated epithelia of bronchial epithelium and weaker, but present, staining in distal alveolar epithelia (Fig. 1 *A–C*). Lung alveolar endothelial, inflammatory, and stromal cells were also positive for LIMD1 expression (data not shown). In agreement with IHC results, Western blot analysis of protein extracts from primary human cell cultures enriched for bronchial epithelia cells (HBECs) or small airway epithelia cells (SAECs) (10) revealed that both epithelia expressed LIMD1 albeit at different levels: HBECs express higher levels than SAECs (Fig. 1 *D* and *E*). Of note, one of the established HBEC cell lines did not express LIMD1 protein.

LIMD1 Expression Is Reduced in the Majority of Lung Cancers Compared with Matched Normal Tissue. We next screened 2 sets of human lung tumors on a tissue microarray (TMA) slide for level of LIMD1 expression, by IHC, and compared this to normal control lung tissue TMA. Tumor expression of LIMD1 was

Author contributions: T.V.S., E.M., and G.D.L. designed research; T.V.S., A.A.-A., D.E.F., L.D., T.Q.d.A.V., Y.Z., H.S.N., T.M.W., A.G.N., Q.Z., A.K., I.S., E.M., and G.D.L. performed research; T.V.S. and G.D.L. contributed new reagents/analytic tools; T.V.S., A.A.-A., D.E.F., L.D., J.O., E.M., and G.D.L. analyzed data; and T.V.S., L.D., and G.D.L. wrote the paper.

The authors declare no conflict of interest.

This article is a PNAS Direct Submission.

[1]A.A.-A. and D.E.F. contributed equally to this work.

[2]To whom correspondence should be addressed. E-mail: glongmor@dom.wustl.edu.

This article contains supporting information online at www.pnas.org/cgi/content/full/0805003105/DCSupplemental.

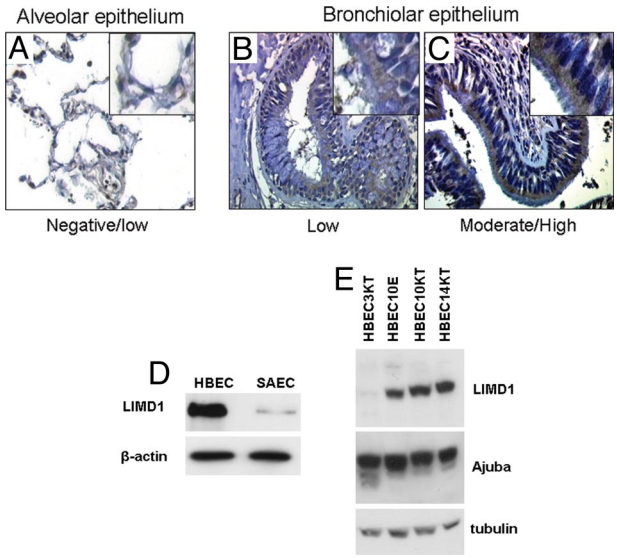

Fig. 1. LIMD1 expression in normal human lung tissue and cells. (*A–C*) Representative examples of anti-LIMD1 mAb staining of normal human alveolar (*A*) and bronchiolar epithelium (*B* and *C*). Examples of the different levels of staining for the TMA cores used for scoring are indicated. (*D*) Primary differentiated HBECs together with primary SAECs were immunoblotted for LIMD1 expression. (*E*) Immortalized HBEC lines were immunoblotted for both LIMD1 and Ajuba expression. β-actin and tubulin were used as controls for protein input levels.

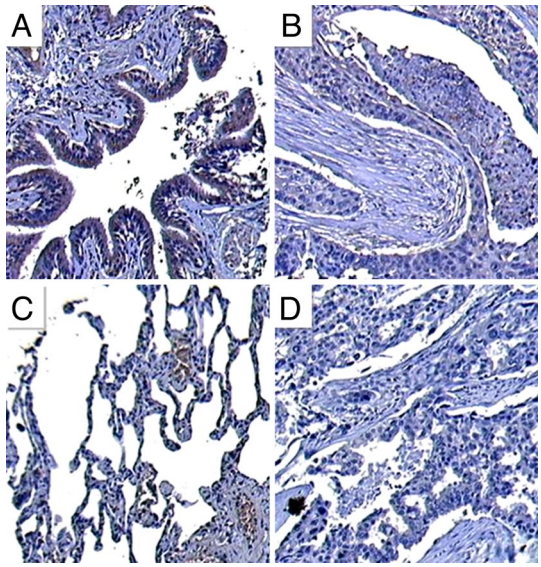

Fig. 2. LIMD1 expression in human lung cancer. Immunohistochemically stained lung normal bronchiolar tissue (*A*) and normal alveolar tissue (*C*) with matched adjacent squamous cell carcinoma tissue section (*B*) and matched adjacent adenocarcinoma section (*D*), respectively. Original magnification was 100×.

consistently weaker (Fig. 2, and Tables 1 and 2). The majority of SQC had statistically significant less LIMD1 staining compared with all normal bronchial tissue (Fig. 2, Tables 1 and 2, and Table S1). However, LIMD1 expression in ADC compared with matched adjacent normal alveolar epithelia was not significantly different (Fig. 2, Tables 1 and 2, and Table S1). But LIMD1 expression in normal small airway epithelia and matched tumor-free adjacent alveolar tissue was weak. When LIMD1 mRNA levels were determined and contrasted between ADC and adjacent normal alveolar epithelia, normal alveolar epithelia expressed higher levels of LIMD1 mRNA relative to tumor (9). In addition, as will be seen later in mice lacking *Limd1* ADC formation by oncogenic K-Ras is dramatically enhanced. These data lead us to suggest that, as is the case for SQC, LIMD1 expression is also likely lost or decreased in ADC.

***LIMD1* Undergoes Genetic Deletion and LOH in Human Lung Cancers.** Decreased expression of LIMD1 in lung cancers could result from acquired coding region mutations, alteration in gene copy number, LOH or epigenetic modifications of transcriptional regulatory regions. To address these possibilities we interrogated the recently published NHGRI-sponsored tumor sequencing project (TSP) dataset of ADC tumor and matched normal DNA (3). Sequencing of all 8 exons and intron-exon boundaries of *LIMD1* in 188 ADC samples revealed no mutations, whereas analysis of gene copy number in 357 matched samples from the TSP ADC set revealed that deletions in the *LIMD1* gene occurred in 32% of samples (Fig. 3*A*). For other evaluated genes in the C3CER1 region *LIMD1* was one of the most commonly deleted genes (Fig. 3*A*). Furthermore, *LIMD1* was deleted more commonly than known lung TSGs (p53 at 17p13) or strongly implicated TSGs (RASSF1A at 3p21.3) (Fig. 3*B*). LOH analysis for 178 interpretable samples revealed that in 12% of these tumors *LIMD1* had undergone LOH. The low percentage gene deletion for *RB1* and higher deletion percentage for *LIMD1* (Fig. 3) is reminiscent of the inverse correlation between RB and p16 (*INK4*) inactivation in both SCLC and NSCLC samples (11) that demonstrated that *RB1* and *INK4* were part of a single pathway where either component (but not both) needed to be inactivated. Therefore, with respect to the corepressor role LIMD1 has with RB (9), loss of *LIMD1* may affect RB tumor suppressive pathways without the need for *RB1* inactivation.

***LIMD1* Is Epigenetically Inactivated via Promoter Hypermethylation in Human Lung Tumors.** Because 75 and 79% of SQC and ADC, respectively, exhibited reduced LIMD1 protein levels whereas only 32% and 12% of ADC in the NHGRI TSP set had evidence of gene deletion or LOH respectively, we asked whether *LIMD1* also underwent epigenetic silencing (through promoter hypermethylation) that could account for the remaining 30–35% of

Table 1. LIMD1 expression on lung cancer

LIMD1	SQC, n, %	ADC, n, %	SCC, n, %	MEC, n, %	Carcinoid, n, %	Total, n
Negative	20 (25)	8 (13)	8 (33)	3 (37.5)	1 (7)	40
Low	39 (50)	39 (66)	15 (63)	5 (62.5)	9 (64)	107
Moderate/High	20 (25)	13 (21)	1 (4)	0 (0)	4 (29)	38
Total	79 (100)	60 (100)	24 (100)	8 (100)	14 (100)	185

Tumors were stained by using the mAb 3F2/C6 immunohistochemically utilizing the avidin-biotin peroxidase method. Cores are scored as Negative (no staining), Low (weak staining), or Moderate/High (strong staining) on a random collection of lung tumors constructed on a TMA block. SQC, squamous cell carcinoma; ADC, adenocarcinoma; SCC, small cell carcinoma; MEC, mucoepidermoid carcinoma.

Table 2. Distribution of LIMD-1 expression on the squamous (SCQ) and adenocarcinomas (ADC) arrays and their corresponding normal lung tissue

LIMD-1	SQC, n, %	ADC, n, %	Alveolar tissue, n, %	Bronchial tissue, n, %
Negative	6 (18)	4 (12)	36 (58.1)	0 (0)
Low	21 (64)	20 (61)	26 (41.9)	3 (37.5)
Moderate/High	6 (18)	9 (27)	0 (0)	5 (62.5)
Total	33 (100)	33 (100)	62 (100)	8 (100)

Sections were stained by using the mAb 3F2/C6 immunohistochemically utilizing the avidin-biotin peroxidase method. Cores are scored as Negative (no staining), Low (weak staining) or Moderate/High (strong staining).

tumor samples with decreased LIMD1 expression. Using a genome browser, we identified a CpG island at −1299 to −439 from the start site of *LIMD1* (Fig. 4*A*). To test whether this region contained promoter activity, a fragment corresponding to −2039 to −10 (WT-P), relative to the ATG initiation codon, was cloned into the pGL4-basic vector and luciferase assays performed. WT-P was found to be active in all cell lines tested; lung ADC cell line A549 (28-fold), breast epithelial cell line MDA-MB435 (60-fold), and the osteosarcoma cell line U2OS (380-fold) compared with empty pGL4 vector control (Fig. 4*A*). We next generated a series of deletion mutants in WT-P upstream from the putative TATA box (−468). The Δ1−P (−1539 to −10) promoter displayed higher activity than WT-P, indicating that the region between −2039 and −1539 contained a negative regulatory element (Fig. 4*A*). Further deletions Δ2−P (−1539 to −1299) did not result in loss of promoter activity, compared with Δ1−P. Deletion of nucleotides −1299 to −439 (Δ3−P), that included the CpG island, reduced promoter activity dramatically in all cell lines tested (Fig. 4*A*). This analysis indicated that the core region of the basal promoter of the human *LIMD1* gene is located within the region −1299 to −439. Through progressive small internal deletions in −1299 to −439 promoter region we identified a 21-bp region (IΔ5: −727 to −706) that appeared to be responsible for the majority of transcriptional activity (Fig. 4*A*).

We next determined the CpG methylation status of the 21 bp IΔ5 promoter region in 48 sets of paired lung tumor and matched adjacent normal lung, by bisulphite sequencing. Of the 48 pairs, 38 gave informative data. Ten of the 38 (26%) showed increased promoter methylation in tumors, specifically at the fourth CpG dinucleotide (Fig. 4*B*). Only 3 normal controls had evidence of promoter methylation and in all cases this was partial (Fig. 4*B*).

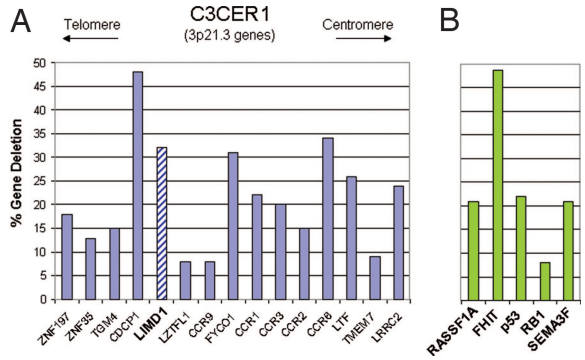

Fig. 3. *LIMD1* gene deletion in human lung cancer. (*A*) Histogram showing the percentage gene deletion for the indicated C3CER1 gene cluster as determined by interrogation of the NHGRI-sponsored TSP dataset of ADC tumor and matched normal DNA (3). Indicated genes are arranged relative to their 3p21.1 spatial location with respect to the 3p telomere and centromere. *LIMD1* is highlighted by cross-hatched pattern. (*B*) For reference and comparison other indicated known TSG (p53, Rb) and putative 3p TSG (*RASSF1A*, *FHIT*, and *SEMA3F*) percentage gene deletions are shown.

Of tumors with increased methylation 86% of these had corresponding reduced LIMD1 mRNA expression in tumors (Fig. S1). Indeed within this tumor/normal set 78% of tumors had evidence for decreased mRNA expression relative to normal adjacent lung, as detected by qRT-PCR (Fig. S1).

To confirm that promoter hypermethylation could contribute to reduced *LIMD1* gene expression in tumors we determined the methylation status of the IΔ5 promoter region in U2OS (expresses LIMD1 protein) and MB435 (do not express LIMD1 protein) cells (Fig. 4*D*). All 4 CpG dinucleotides were methylated in MB435 cells whereas none were methylated in U2OS cells (Fig. 4*C*). These cell lines were then treated with the DNA methylase inhibitor 5-Aza-2′-deoxycytidine (5 Aza-CdR) for 5 days. 5-Aza-CdR treatment resulted in the reexpression of LIMD1 protein in MB435 cells without affecting LIMD1 expression in U2OS cells (Fig. 4*D*).

In summary, expression of LIMD1, a 3p21.3 gene, in human lung cancers is down regulated in the majority of human lung tumors examined. The total loss of expression (75% for SQC and 79% for ADC) as determined by IHC correlates closely to the genetics of *LIMD1* in human lung cancers: gene deletion (32%), LOH (12%), and epigenetic silencing (26%).

***LIMD1* Loss Renders Mice Susceptible to Lung Chemical Carcinogens.** To test experimentally whether LIMD1 can function as a TSG in lung cancer development, in vivo, we made use of *Limd1*$^{-/-}$ mice (12) and asked whether the incidence of cancer increased in mice lacking LIMD1 after exposure to an environmental carcinogen or a second genetic event (13, 14). We challenged *Limd1*$^{-/-}$ and control littermates to the carcinogen urethane (13, 15). *Limd1*$^{-/-}$ mice developed more tumors and increased lung tumor volume in response to urethane (Fig. 5 *A* and *B*). The number of tumors observed in both wt controls and Limd1$^{-/-}$ mice were low because C56BL/6 mice are a relatively resistant strain and only a single dose of urethane was given (16).

Cooperativity Between K-Ras and LIMD1 in Lung Tumor Suppression. In a genetic approach, *Limd1*$^{-/-}$ mice were bred to mice that will express a single copy of oncogenic *K-Ras*^{G12D} (LA1 allele) (17). *K-Ras*^{G12D} (LA1) mice develop multiple lung adenomas and succumb to adenocarcinomas over a well-described temporal scale. *Limd1*$^{-/-}$;*K-Ras*$^{G12D+/-}$ mice had greatly increased tumor incidence (number of tumors per lung) and tumor promotion (total volume of tumor per lung or average tumor volume) at both 13 and 16 weeks of age (Fig. 5 *C* and *D* and Fig. S2). *Limd1* also showed a gene dosage effect as analysis of *Limd1*$^{+/-}$;*K-Ras*^{G12D} mice revealed a statistically significant different and intermediate value in tumor number and total tumor volume per lung compared with *Limd1*$^{+/+}$;*K-Ras*^{G12D} and *Limd1*$^{-/-}$;*K-Ras*^{G12D} mice (Table S2). Histologically, like *K-Ras*^{G12D} mice, *Limd1*$^{-/-}$;*K-Ras*^{G12D} mice developed both adenomas and adenocarcinomas (Fig. 5*E*). Although the number of adenocarcinomas present in the lungs of *Limd1*$^{-/-}$;*K-Ras*^{G12D} mice increased with age of analysis and tumor size, we did not observe any significant difference in the ratio of adenomas/adenocarci-

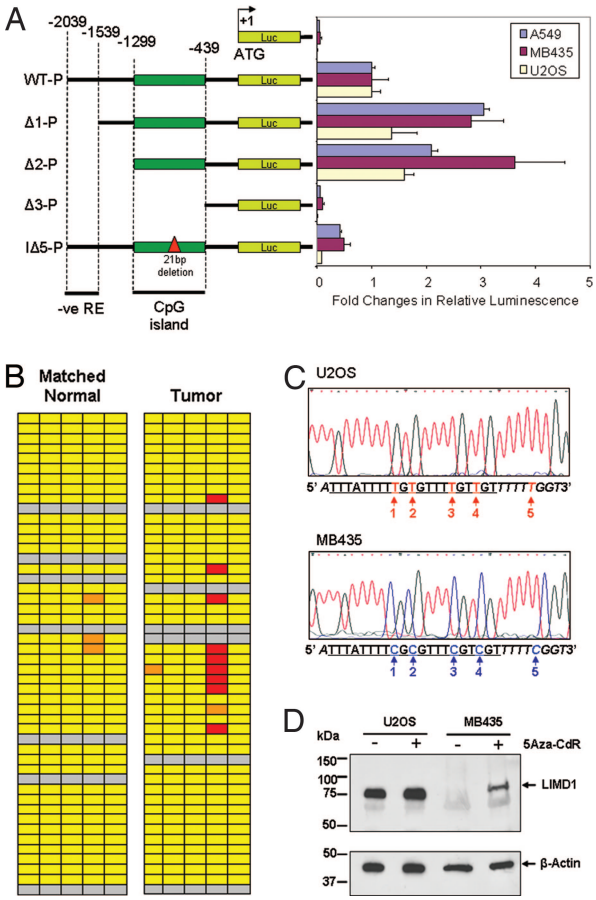

Fig. 4. *LIMD1* promoter characterization and bisulphite sequence analysis of the human *LIMD1* gene promoter. (*A*) Reporter analysis of human *LIMD1* gene promoter deletion constructs. The 5′−deleted promoter segments (Δ1−P, 2−P, and 3−P) and the 21-bp internal deletion−5 (−727 to −706) (IΔ5−P, red) were generated as described in *Materials and Methods*. The indicated cell lines were cotransfected with the various promoter-reporter vectors and a Renilla luciferase expression control vector. The resulting firefly luciferase activity was then normalized to Renilla luciferase activity and the relative values are presented as the fold-changes over the activity of the wild-type *LIMD1* promoter in pGL4.10 (WT-P). Relative luminescence values represent the mean ± SD of 3 independent experiments. (*B*) Genomic DNA from 48 lung tumor and matched normal controls was extracted and bisulphite sequenced across the critical IΔ5 promoter region to assess differences in methylation status. Each box represents the indicated 5 CpG dinucleotides within the sequenced analyzed and the core IΔ5 sequence is underlined. Matched normal and tumor tissue pairs where bisulphite sequencing failed for one or both samples were omitted from subsequent analysis. *Yellow*, unmethylated; *orange*, partially methylated; *red*, methylated and gray, no data. (*C*) Genomic DNA from LIMD1 expressing and nonexpressing U2OS and MB435 cells underwent bisulphite sequencing of the IΔ5 promoter region (21bp underlined). Methylated cytosines are resistant to the initial bisulphite treatment, so are conserved after sequencing (red), whereas unmethylated cytosines are converted to uracil and subsequently appear as thymine when sequenced (blue). (*D*) U2OS and MB435 cells were treated with (+) and without (−) the DNA methylation inhibitor 5-Aza-2′-deoxycytidine for 5 days, cells were lysed and LIMD1 western blot analysis was performed, with β-actin as a loading control.

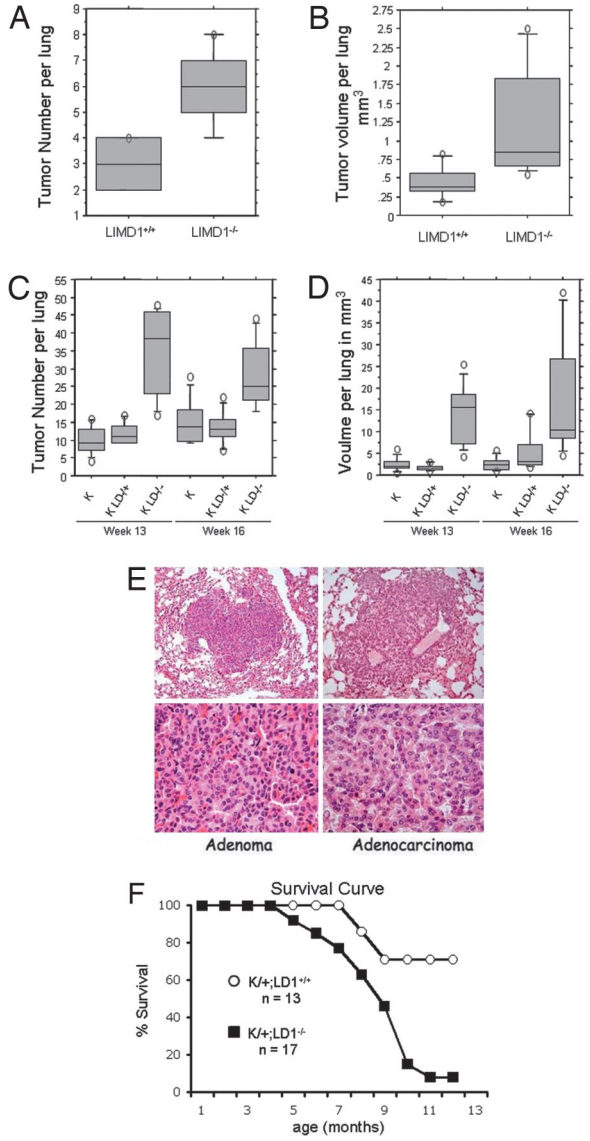

Fig. 5. Deletion of *Limd1* accelerates lung tumor initiation and promotion when challenged with an environmental carcinogen or secondary genetic factor. (*A* and *B*) Limd1$^{-/-}$ mice have an increased propensity to develop lung tumors in a chemical carcinogenesis model. Limd1$^{-/-}$ (n = 12) or littermate Limd1$^{+/+}$ (n = 9) mice, in a C57BL/6 background, were injected with urethane at 21 days and killed 6 months later. Number of tumor per lung (*A*) and total tumor volume per lung (*B*) were determined and plotted. Box plot: Shaded box, middle 50% of the dataset. Line in box, median value of the dataset; Vertical bars, minimum data values; Circles, outliers. All differences were statistically significant P value <0.05, Student t test. (*C* and *D*) Deletion of *Limd1* accelerates lung tumor initiation and promotion in K-Ras^{G12D} mice. Limd1$^{-/-}$ mice were bred to K-Ras^{G12D}(LA-1 allele) mice. Both alleles were in a C57BL/6 background. Mice were killed at 13 weeks (Limd1$^{+/+}$;K-Ras$^{G12D+/-}$ n = 9; Limd1$^{+/-}$;K-Ras$^{G12D+/-}$ n = 5; Limd1$^{-/-}$;K-Ras$^{G12D+/-}$ n = 10) and 16 weeks (Limd1$^{+/+}$;K-Ras$^{G12D+/-}$ n = 8; Limd1$^{+/-}$;K-Ras$^{G12D+/-}$ n = 9; Limd1$^{-/-}$;K-Ras$^{G12D+/-}$ n = 9). Tumor number per lung (*C*) and total tumor volume per lung (*D*) were determined and plotted. All differences were statistically significant P value <0.02, Student t test. Box plot: Shaded box, middle 50% of the dataset. Line in box, median value of the dataset; Vertical bars, minimum data values; Circles, outliers. (K) *K-RasG12D*$^{+/-}$ genotype, LD, *Limd1* genotype. (*E*) Representative histological analysis of tumors present in K-RasG12D;Limd1$^{-/-}$ mice H&E stained. (*F*) Deletion of *Limd1* increases mortality in K-RasG12D mice. Percentage survival in mice carrying the indicated genotype is shown by Kaplan–Meier plots. Survival of mice over the indicated follow-up period is shown as the percentage number of mice alive/total mice analyzed for each genotype.

nomas between *Limd1*$^{-/-}$;*K-Ras*^{G12D} mice and *K-Ras*^{G12D} mice, at 10, 13, or 16 weeks of age. We also monitored *Limd1*$^{-/-}$;*K-Ras*^{G12D} and *Limd1*$^{+/-}$;*K-Ras*^{G12D} mice survival over a 12-month period. Kaplan–Meier plots clearly show that loss of *Limd1* increased mortality (Fig. 5*F*).

In summary, these mouse experiments show that loss of *Limd1* renders mice susceptible to both chemical carcinogen and cooperating oncogenic events for the development of lung adeno-

carcinoma, and provide experimental proof that directly corroborates the human IHC and genetic analysis indicating LIMD1 could indeed be a human tumor suppressor gene in the development of lung cancer.

LIMD1 is an actin-associated protein that localizes to E-cadherin-dependent cell–cell adhesive junctions and integrin-dependent ECM adhesive sites (18), influences inflammatory responses (12), yet also translocates in/out of the nucleus where it has been shown to function as an RB corepressor (9). As such, LIMD1 serves to communicate cell extrinsic environmental events with nuclear responses. Whether it is the cell surface adhesive functions of LIMD1, cytosolic signaling function, nuclear functions, or some combination that contribute to lung tumor suppression, and how, remains to be determined. Finally it will be critical to determine whether the level of LIMD1 expression in human lung tumor samples has clinical prognostic value.

Materials and Methods

Tissue Culture. Primary HBECs were purchased from Clonetics and cultured and differentiated according to published methods (19). Briefly, undifferentiated HBECs were cultured in growth-factor supplemented bronchial epithelial basal medium (Cambrex). SAECs were cultured in small airway basal media (SABM) supplemented with growth factors purchased as SABM singlequots (Cambrex) until 70% confluent. Fresh media was added every 48 h.

Tissue Microarrays and Immunohistochemistry. Tissue microarray slides were obtained from Tissue Array Network. Slides were baked at 60°C for 2 h before staining with a standard streptavidin-biotin-peroxidase protocol for immunohistochemistry. Briefly, slides were dewaxed in xylene (2 × 10 min) and rehydrated in 3 grades of ethanol (99%, 90%, then 70%) for 10 min each. Endogenous peroxidase activity was blocked by immersing the slides in a 0.03% solution of H_2O_2 in methanol for 25 min. Heat-induced epitope retrieval (HIER) was done by using an 800-Watt rotary microwave oven in 10 mm sodium citrate buffer (pH 6.0) for 10 min on high power, then for 10 min on low power. Slides were cooled and washed with Tris-buffered saline (TBS; 0.05 mol/L Tris-HCl, 0.15 mol/L NaCl, pH 7.6) for 10 more minutes. To reduce nonspecific adsorption of antibodies, slides were incubated with normal swine serum (NSS, Dako), diluted 1:20 in TBS for 10 min. The test sections were incubated with anti-LIMD1 antibody for 1 h at room temperature. Negative control sections were incubated with NSS. After a thorough wash with TBS, 100 μl of a biotinylated anti-mouse antibody, diluted 1:100 (Dako) was applied for 30 min, followed by another TBS wash, then 100 μl of a preprepared streptavidin-biotin/ peroxidase complex solution for 60 min. Color was developed by using 3,3′-diaminobenzidine (Dako), enhanced with 0.5% cupper sulfate solution, and then counterstained with Mayer's hematoxylin solution (Dako) for 1 min. Staining intensity was scored as negative (no staining), weak, moderate, or high.

Human Lung Tissue Sample Collection and Storage. One sample each of fresh tumor tissue and normal lung parenchyma distant from tumor were collected from patients undergoing operative resection of lung cancer at the Royal Brompton Hospital. Both samples were snap-frozen in isopentane and stored at −80°C. Specific consent for usage of tissue from operation that would otherwise not for diagnosis was obtained from patients and the study was approved by the Brompton, Harefield and NHLI Research Ethics Committee, U.K.

Human Genetic Analysis. *SNP array data preprocessing.* The dChip software was used to read Affymetrix 250k Sty array CEL files and to export background-subtracted probe values by using the PM -only option. For each spot on the array and each probe set (i.e., each SNP), $\log_2$ of the average of PM intensities across 12 probes was used as the basic measurement, *S*. For each array, *S* values for 238,304 SNPs were scaled to have a mean of 0 and a variance of 1 by normalization. For each SNP and each sample pair, DNA copy number was estimated based on the difference of *S* between tumor and normal samples (i.e., $\log_2$ ratio of the tumor and normal intensities).

For genes with >10 SNPs, all SNPs within the gene were used to compute the DNA copy number of the gene. For genes with <10 SNPs, the average intensity of the 10 SNPs closest to the most centrally localized SNP, within or outside of the gene, was used to calculate the DNA copy number of the gene to minimize the risk of higher variability associated with a small number of SNPs. For each pair, mean and variance of CN values of 28 SNPs within LIMD1 were calculated, and *t* test was used to test whether the CN mean of LIMD1 is zero. The *P* value was obtained from the *t* distribution. Significant amplification and deletion were defined as below:

Amplification: Mean >0 and $P < 0.01$

Deletion: Mean <0 and $P < 0.01$

DNA methylation analysis. Methylation of the CpG island within the *LIMD1* promoter was analyzed by using bisulphite sequencing. Genomic DNA from lung tumor tissue and matched normal lung tissue from 48 patients was extracted and 500 ng of DNA from each sample bisulphite treated by using EZ DNA Methylation-Gold Kit (Zymo Research). 10 ng of each treated DNA was amplified by using the nonmethylation discriminatory primers 5′ GGYGYGGGTTYGGGAYGTGTAGAGTYGG (forward) and 5′ CTAAAACTA-ACRACCCATTATCCRATAAC (reverse), corresponding to −787 to −648 of the *LIMD1* relative to the $A^{(+1)}$TG. Conditions for the PCR were 1 cycle at 94°C for 3 min, 40 cycles at 94°C for 15 s, at 61.5°C for 1 min, and at 72°C for 30 s with a final elongation at 72°C for 2 min. The 149-bp products were purified by gel extraction (Qiagen) and sequenced by using the same forward primer. Unmethylated and methylated genomic DNA from LIMD1 expressing U2OS and non-LIMD1 expressing MB435 cells, respectively, were used as controls. MB435 and U2OS cells were treated with 100 μM 5-Aza-2′-deoxycytidine (Sigma), an inhibitor of DNA methylation, for 5 days, with drug and media changes each day.

For LOH analysis and tumor mRNA expression, see *SI Text*.

Promoter Analysis. The *LIMD1* promoter region (LPR) and gene was examined by using the UCSC Genome Browser software interface facility (http://genome.cse.ucsc.edu/cgi-bin/hgGateway) and the March 2006 human reference sequence (National Center for Biotechnology Information Build 36.1) produced by the International Human Genome Sequencing Consortium. Briefly, the upstream −2049 bp relative to the translation initiating $A^{(+1)}$TG of the LIMD1 reference sequence LIMD1 (uc003coq.1) at chr3:45611327–45697759 to −10 base pairs relative to the initiating ATG was cloned from genomic DNA isolated from normal bronchial epithelial tissue by using the 5′-primer (LPP-15′)CGG*GGTAC*CCAGGCACTTGGCATACAGATATGG (LPP-1–5′) and the 3′-primer (LPP-23′) GGG*AAGCTT*AGGTGTCCGGGCCTAGCCCAGG (LPP-2–3′) which incorporated the *Kpn*I and *Hin*dIII restriction sites respectively. The amplicon was then cloned into the pGL4.10[*luc2*] (Promega) reporter vector for analysis. A series of constructs containing variable lengths of the human LIMD1 promoter were then generated by PCR (all primer sequences available on request). All LIMD-1 promoter constructs were cloned into pGL4.10[luc2] vector by using restriction digested with K*pn*I and H*ind*III to generate luciferase reporter constructs.

The CpG island was predicted by using the UCSC Genome Browser software interface facility by searching the sequence 1 base at a time, scoring each dinucleotide (+17 for CG and −1 for others) and identifying maximally scoring segments. Each segment was then evaluated for the following criteria: GC content of 50% or greater; length >200 bp; ratio >0.6 of observed number of CpG dinucleotides to the expected number on the basis of the number of Gs and Cs in the segment. The CpG count is the number of CG dinucleotides in the island. The Percentage CpG is the ratio of CpG nucleotide bases (twice the CpG count) to the length. The ratio of observed to expected CpG is calculated according to the formula cited in Gardiner-Garden *et al.* (19).

A tandem array of 10 internal promoter deletions IΔ1−P to IΔ10−P within a highly conserved region (−917 to −574) within the *LIMD1* promoter CpG island (−1299 to −439) were created by a nested PCR (primer sequences available on request) with pGL4.10[luc2] −2049 to −10 bp hLIMD-1 promoter as template. PCR products were cloned into pGL4.10[luc2] vector by using *Kpn*I and *Hin*dIII restriction sites and the sequence verified by sequencing analysis (Biopolymer Unit, Queen's Medical Center, University of Nottingham).

Protein Analysis. For detection of LIMD1 protein, we used the described mouse monoclonal antibody raised against human LIMD1 protein (3F2/C6), the epitope of which is amino acids 144–214 (10). To normalize signals, filters were reprobed with antibodies against β-actin where indicated.

Statistical Analysis. Statistical analyses were performed by using GraphPad Prism 5.0. Categorical variables were compared by using cross-tabulation and Pearson's χ^2 test. One-way ANOVA test was used to analyze the difference between sample means (http://www.graphpad.com/articles/interpret/ANOVA/one way.htm). A post hoc test for trend was implemented to test whether such difference was significant in an ordinal manner. Acceptance of statistical significance was based on an alpha of ≤0.05.

Mouse Lung Cancer Models. ***Chemical carcinogenesis*** Mice (C57BL/6 genetic background) were injected once with urethane, 1 mg/g, i.p., at 3 weeks of age. Six months later mice were killed, lungs dissected, fixed in Tellyesniczky solution

overnight, and then 75% EtOH was added. Tumor number and diameter (mm) were determined in a blinded manner, under a dissecting microscope. Individual tumor volumes were determined based on the formula: $V(mm^3) = 4/3\Pi r^3$, and reported as total tumor volume per lung.

K-Ras cooperativity. Limd1$^{-/-}$ mice were bred to K-Ras^{G12D} (LA-1 allele) mice. Both alleles were on a C57BL/6 genetic background. At 13 and 16 weeks of age, mice were killed, lungs dissected, fixed in Tellyesniczky solution overnight, and then 75% EtOH. Tumor number and diameter (mm) were determined in a blinded manner, under a dissecting microscope. Individual tumor volumes were determined based on the formula: $V(mm^3) = 4/3\Pi r^3$, and reported as total tumor volume per lung. Mice with evidence of lymphomatous involvement of the lung were excluded from the analysis.

ACKNOWLEDGMENTS. We thank Prof. John Amour and Dr. Jess Tyson for helpful advice and technical assistance, Dr. Dimitris Lagos for help with statistical analyses, the Department of Thoracic Surgery, Royal Brompton Hospital, led by Professor P. Goldstraw, for help in collection of samples of lung tumors, Dr. J. Minna (University of Texas Southwestern, Dallas) for providing human HBEC cell lines, and Dr. Ming You for helpful discussions. This work was supported by British Lung Foundation Grant P05/2 (to T.V.S.) and National Institutes of Health Grants CA106496 and GM080673 (to G.D.L.).

1. Ji L, Minna JD, Roth JA (2005) 3p21.3 tumor suppressor cluster: Prospects for translational applications. *Future Oncol* 1:79–92.
2. Kost-Alimova M, Imreh S (2007) Modeling non-random deletions in cancer. *Semin Cancer Biol* 17:19–30.
3. Weir BA, *et al.* (2007) Characterizing the cancer genome in lung adenocarcinoma. *Nature* 450:893–898.
4. Kiss H, *et al.* (1999) A novel gene containing LIM domains (LIMD1) is located within the common eliminated region 1 (C3CER1) in 3p21.3. *Hum Genet* 105:552–559.
5. Petursdottir TE, *et al.* (2004) Interstitial deletions including chromosome 3 common eliminated region 1 (C3CER1) prevail in human solid tumors from 10 different tissues. *Genes Chromosomes Cancer* 41:232–242.
6. Imreh S, *et al.* (1994) Nonrandom loss of human chromosome 3 fragments from mouse-human microcell hybrids following progressive growth in SCID mice. *Genes Chromosomes Cancer* 11:237–245.
7. Zabarovsky ER, Lerman MI, Minna JD (2002) Tumor suppressor genes on chromosome 3p involved in the pathogenesis of lung and other cancers. *Oncogene* 21:6915–6935.
8. Imreh S, Klein G, Zabarovsky ER (2003) Search for unknown tumor-antagonizing genes. *Genes Chromosomes Cancer* 38:307–321.
9. Sharp TV, *et al.* (2004) LIM domains-containing protein 1 (LIMD1), a tumor suppressor encoded at chromosome 3p21.3, binds pRB and represses E2F-driven transcription. *Proc Natl Acad Sci USA* 101:16531–16536.
10. Shames DS, *et al.* (2006) A genome-wide screen for promoter methylation in lung cancer identifies novel methylation markers for multiple malignancies. *PLoS Med* 3:e486.
11. Otterson GA, Kratzke RA, Coxon A, Kim YW, Kaye FJ (1994) Absence of p16INK4 protein is restricted to the subset of lung cancer lines that retains wildtype RB. *Oncogene* 9:3375–3378.
12. Feng Y, *et al.* (2007) The LIM protein, Limd1, regulates AP-1 activation through an interaction with Traf6 to influence osteoclast development. *J Biol Chem* 282:39–48.
13. Sharpless NE, *et al.* (2001) Loss of p16Ink4a with retention of p19Arf predisposes mice to tumorigenesis. *Nature* 413:86–91.
14. Wang Y, Zhang Z, Lubet RA, You M (2006) A mouse model for tumor progression of lung cancer in ras and p53 transgenic mice. *Oncogene* 25:1277–1280.
15. Herzog CR, Noh S, Lantry LE, Guan KL, You M (1999) Cdkn2a encodes functional variation of p16INK4a but not p19ARF, which confers selection in mouse lung tumorigenesis. *Mol Carcinog* 25:92–98.
16. Miller YE, *et al.* (2003) Induction of a high incidence of lung tumors in C57BL/6 mice with multiple ethyl carbamate injections. *Cancer Lett* 198:139–144.
17. Johnson L, *et al.* (2001) Somatic activation of the K-ras oncogene causes early onset lung cancer in mice. *Nature* 410:1111–1116.
18. Marie H, *et al.* (2003) The LIM protein Ajuba is recruited to cadherin-dependent cell junctions through an association with alpha-catenin. *J Biol Chem* 278:1220–1228.
19. Gardiner-Garden M, Frommer M (1987) CpG islands in vertebrate genomes. *J Mol Biol* 196:261–282.